Contents lists available at SciVerse ScienceDirect

Journal of Environmental Radioactivity

journal homepage: www.elsevier.com/locate/jenvrad



Assessment of natural radioactivity levels and their relationship with soil characteristics in undisturbed soils of the northeast of Buenos Aires province, Argentina

M.L. Montes, R.C. Mercader, M.A. Taylor, J. Runco, J. Desimoni*

Departamento de Física, Facultad de Ciencias Exactas, Universidad Nacional de La Plata, Instituto de Física La Plata-CONICET, CC 67, 1900 La Plata, Argentina

ARTICLE INFO

Article history:
Received 18 May 2011
Received in revised form
26 August 2011
Accepted 12 September 2011
Available online xxx

Keywords: Natural radioactivity Soil properties Fe phases Mössbauer spectroscopy

ABSTRACT

Surface and depth profile concentrations (down to 50 cm) of ²³²Th chain, ²²⁶Ra, and ⁴⁰K radionuclides were determined in undisturbed coastal and inland soils of La Plata city region, Argentina, through their gamma-ray activity using a high-purity Ge detector spectrometer. These results were compared with superficial activities determined in soils from the surroundings of the Centro Atómico Ezeiza (Ezeiza Atomic Center) located in Ezeiza, Buenos Aires Province, Argentina. The hyperfine and magnetic Fe phase's properties of soil profiles were characterized by Mössbauer spectroscopy, magnetic hysteresis loops and AC magnetic susceptibility.

No dependence of the activity of the ²³²Th natural chain on depth was found, whereas variations for ²²⁶Ra and ⁴⁰K activities were observed. Positive correlations, determined by the Pearson correlation coefficients, were established between ⁴⁰K, ²²⁶Ra and ²³²Th activity concentrations for the whole set of soil samples.

The annual external equivalent dose for adults was similar for La Plata and Ezeiza regions, with average values of 0.08 \pm 0.01 mSv and 0.06 \pm 0.02 mSv, respectively.

The thermal dependence of the AC magnetic susceptibility revealed the existence of magnetite and hematite. The Mössbauer spectra of all soils were made up of signals associated with α -Fe₂O₃, a paramagnetic relaxation component, and Fe³⁺ and Fe²⁺ doublets. In addition, the spectra of inland soils revealed the presence of Fe₃O₄. A negative correlation was found between the activity concentrations and the α -Fe₂O₃ and Fe₃O₄ relative fractions, whereas a positive correlation was found between the Fe³⁺ relative fraction and the ⁴⁰K activity.

© 2011 Elsevier Ltd. All rights reserved.

1. Introduction

Soil is the most important source of natural radiation, containing trace quantities of radioactive elements, like ²³⁸U, ²³²Th, their daughter products, and ⁴⁰K, whose concentrations depend on the local geology of each region (UNSCEAR, 2000). The assessment of the activity concentrations of natural radionuclides is of particular importance because it embodies an important contribution to the external dose of the population. In this frame, the United Nations Scientific Committee on the Effects of the Atomic Radiation (UNSCEAR) provides a direct correlation between the activity of ²³⁸U, ²³²Th and ⁴⁰K of soils and the external doses absorbed by the population (UNSCEAR, 2000). The radionuclides present in soils can pass on to the food chain and the air, contributing to the internal

dose received by the population. Human activities can modify the natural concentrations of radionuclides by the release of residues or effluents to the environment, which cause the accumulation of radioactive elements. In these cases, local factors are not easy to take into account, since natural background varies substantially within and between countries (IAEA, 2003). The principles governing long-term environmental and human protection need to take into account the natural background. In the case of naturally occurring radionuclides, there is always a local background level against which cleanup goals and/or regulatory target values should be evaluated.

In Argentina, UNSCEAR reports only the activity concentration of ⁴⁰K in soils, in the range from 559 Bq/kg to 773 Bq/kg (UNSCEAR, 2000; UNSCEAR, 2008). More recently, ²²⁶Ra (73 Bq/kg) and ⁴⁰K (740 Bq/kg) data of semi-natural grassland soils from the central part of the country (Province of San Luis) have been assessed (Jury Ayub et al., 2008).

^{*} Corresponding author. Fax: +54 221 4252006. E-mail address: desimoni@fisica.unlp.edu.ar (J. Desimoni).

Because of the lack of systematic information on the natural activity baselines, we have started a long-term project to contribute to the gamma emitter activity determination in undisturbed soils and have assessed the annual external equivalent dose. Megumi et al. (1988) and Suresh et al. (2011) have claimed that the activity concentrations of natural radionuclides may be related to the soil composition, therefore, the radiological profile has been complemented with magnetic (hysteresis loops and AC magnetic susceptibility) and hyperfine (Mössbauer spectroscopy) studies. This technique allows the identification of different Fe phases and the quantification of their relative fractions (Murad, 2010;

Vandenberghe, 1991). The main Mössbauer parameters are the isomer shift, the quadrupole splitting, and the magnetic hyperfine field. Mössbauer parameters of oxides, oxyhydroxides and substituted clays depend on their chemical composition, crystal structure, and magnetic regimes, among other variables. In natural samples, these parameters are influenced by crystal defects, stoichiometry, particle size, or substitution of iron by other atoms. Activity correlations between ⁴⁰K, ²²⁶Ra and ²³²Th have been determined and are discussed as well as the relationship between the activity of the radionuclides and the Mössbauer relative area of the different iron phases.

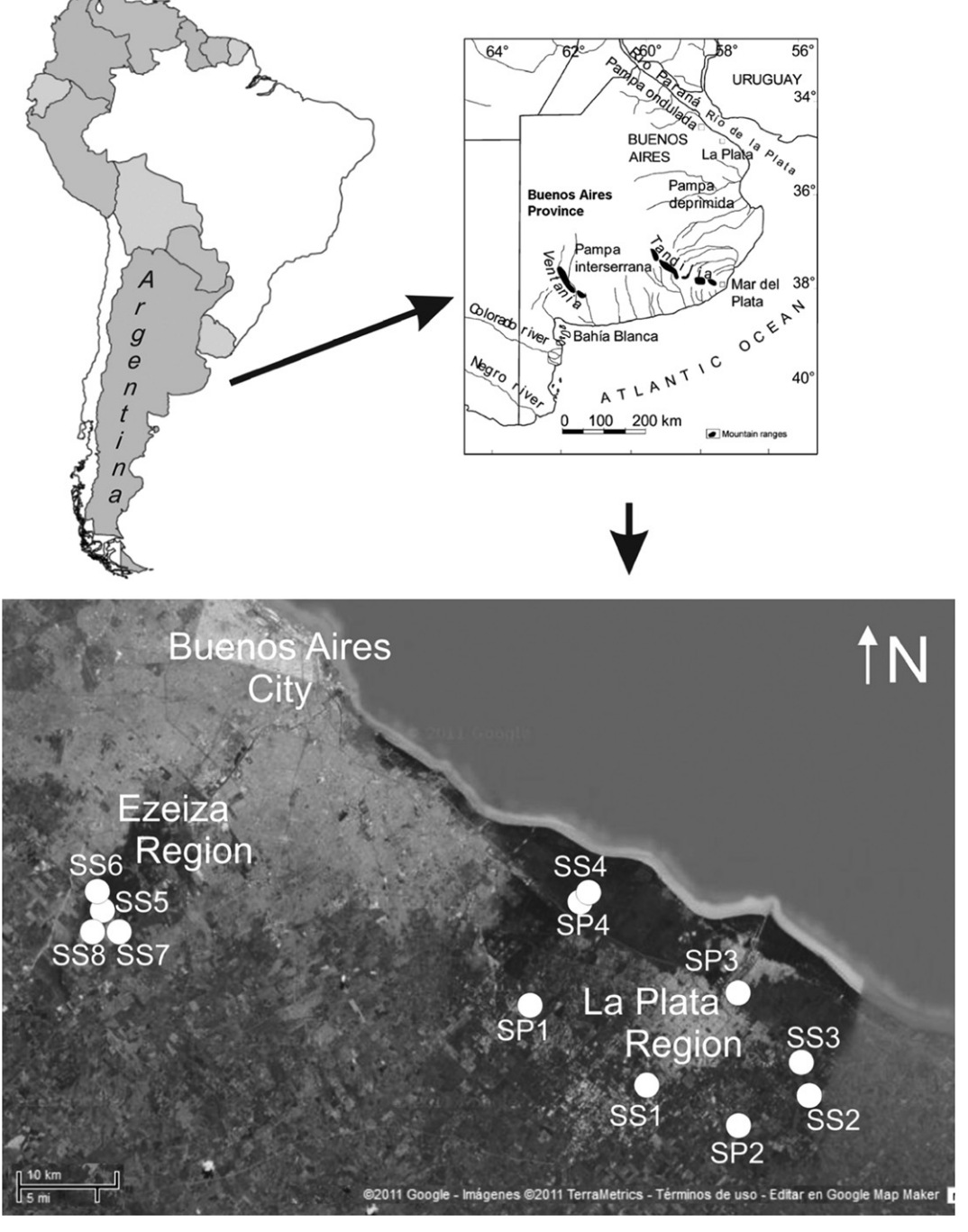


Fig. 1. Location of the sampled soils.

 Table 1

 Locations of investigated soils indicating sample code and monitoring profile.

Sample code	Location	Sampling
SP1	34°54'27.12"S, 58°8'21.90"W	Profile
SP2	35°3′15.66"S, 57°51'12.84"W	Profile
SP3	34°54'8.58"S, 57°55'6.00"W	Profile
SP4	34°48'27.60"S, 58° 5'14.88"W	Profile
SS1	34°59'13.02"S, 57°59'48.30"W	Surface
SS2	35° 0'41.94"S, 57°44'17.28"W	Surface
SS3	34°57'51.24"S, 57°45'39.30"W	Surface
SS4	34°48'5.04"S, 58° 5'2.46"W	Surface
SS5	34°49'40.38''S, 58°35'8.22''W	Surface
SS6	34°49'18''S, 58°35'8.22''W	Surface
SS7	34°50'41.6''S, 58°34'43.7''W	Surface
SS8	34°50'27.7'', 58°45'7.7'' W	Surface

2. Materials and methods

2.1. Studied region

The Province of Buenos Aires is an important agricultural and industrial area. At the north of the province (Lima city), a nuclear power plant, Atucha I, is under operation and a second one is under construction (NASA, 2011). In addition, the *Centro Atómico Ezeiza* (Ezeiza Atomic Center) belonging to the *Comisión Nacional de Energía Atómica* (Atomic Energy National Commission) is located in the Ezeiza densely populated region. In this region there is a nuclear reactor devoted to the development and production of radionuclides used in medical, agricultural and livestock applications. In addition, the center has facilities to manufacture the nuclear power reactor fuel bars and to manage the radioactive waste generated across the country (CNEA, 2011).

In the studied area (Fig. 1), two main geo-morphological units can be differentiated: i) area of estuary-marine influence and ii) area of continental influence, called hereafter coastal and inland soils, respectively. Regarding the topography, the first one is a low plain with a relief plain and plain-convex parallel to the *La Plata River* coast between 0 and 5 m above sea level, covered by marine and fluvial deposits originated by the river discharge and the fluvial transport. Previous studies of soils have reported high clay fraction

(57–70% in surface) in the coastal area (Gimenez et al., 2005; Hurtado et al., 2006a; 2006b). The inland area is a high plain belonging to the Pampa Ondulada, with soft undulations affecting the loessic deposits. The height above the sea is higher than 5 m with main watershed NW-SE with maxima heights of 30 m to the NW and 20 m to the SE, acting as water divisors. In this region, the soils present clay contents from 26 to 35% in surface (Gimenez et al., 2005; Hurtado et al., 2006a; 2006b).

2.2. Sampling

Four undisturbed soils were selected near La Plata city, Province of Buenos Aires, from different areas: (i) inland (SP1 and SP2) and (ii) coastal (SP3 and SP4). The location of the soils is depicted in Fig. 1 and Table 1. The sampling was performed at depths down to 50 cm from the surface, taking samples at approximately 3 cm depth intervals. Surface samples were collected (SS1, SS2, SS3 and SS4 as shown in Fig. 1 and Table 1) in the same areas. In order to evaluate and to compare the soil natural radionuclide activity of La Plata and Ezeiza regions, four superficial samples (0–10 cm) were taken in the neighborhood of the Centro Atómico Ezeiza (SS5, SS6, SS7 and SS8, displayed in Fig. 1 and Table 1).

The samples for radiological analysis were collected with a spade 3 cm high and 30 cm wide, while the samples for Mössbauer spectroscopy measurements were taken with small plastic tubes to avoid Fe contamination.

After collected, the samples were dried at 363 K until no further weight loss could be detected. The samples were subsequently crushed, sieved through a 2 mm mesh without previous separation, and put in the corresponding sample holder. The water concentration of the samples was checked using a Shitmatzu Tg-50 Thermogravimeter heating 5°/min up to 473K in N atm, which yielded a remainder water content lower than 2 wt.%.

2.3. Experimental techniques

For gamma spectroscopy, the soil samples were properly accommodated in a Marinelli-type box (2 L), sealed and kept for

Table 2⁴⁰K, ²³²Th and ²²⁶Ra activities determined for the studied soils. WA = worldwide average values for superficial samples (UNSCEAR, 2008). SLP = average activity in San Luis province. B = average activity in Brazil. U = average activity in Uruguay.

Sample	Depth	²²²⁶ Ra	²³² Th (Bq/kg)	⁴⁰ K (Bq/kg)	Sample	Depth	²²²⁶ Ra	²³² Th	⁴⁰ K (Bq/kg)	Sample	²²²⁶ Ra	²³² Th	⁴⁰ K
code	(cm)	(Bq/kg)			code	(cm)	(Bq/kg)	(Bq/kg)		code	(Bq/kg)	(Bq/kg)	(Bq/kg)
SP1	2.3	30 ± 4	33 ± 6	531 ± 56	SP2	1.8	27 ± 6	35 ± 6	622 ± 66	SS1	27 ± 5	40 ± 6	647 ± 66
	4.4	32 ± 5	35 ± 6	532 ± 52		4.5	29 ± 6	36 ± 6	631 ± 67	SS2	28 ± 7	35 ± 5	576 ± 61
	6.5	33 ± 4	34 ± 5	565 ± 60		7.3	25 ± 5	35 ± 5	615 ± 64	SS3	21 ± 3	30 ± 5	658 ± 70
	9.4	35 ± 5	35 ± 6	568 ± 61		9.5	30 ± 4	38 ± 7	675 ± 70	SS4	61 ± 8	43 ± 6	873 ± 90
	12.1	31 ± 4	32 ± 6	571 ± 54		12.0	30 ± 6	37 ± 5	688 ± 71	SS5	26 ± 5	35 ± 19	644 ± 92
	14.9	37 ± 5	36 ± 5	577 ± 61		15.0	29 ± 7	35 ± 4	649 ± 69	SS6	21 ± 3	27 ± 18	498 ± 87
	18.3	33 ± 4	35 ± 6	576 ± 61		18.8	30 ± 6	35 ± 5	653 ± 67	SS7	20 ± 3	24 ± 15	470 ± 78
	21.3	37 ± 5	39 ± 7	598 ± 62		21.8	31 ± 4	40 ± 6	695 ± 72	SS8	18 ± 3	32 ± 8	547 ± 81
	23.5	38 ± 6	39 ± 6	618 ± 66		25.0	32 ± 6	39 ± 7	723 ± 74				
	25.5	32 ± 4	40 ± 7	684 ± 64		41.5	30 ± 8	42 ± 7	788 ± 81				
	29.3	35 ± 4	45 ± 13	733 ± 73									
	37.3	33 ± 3	41 ± 6	593 ± 59									
	49.0	32 ± 5	42 ± 7	726 ± 69									
SP3	4.0	41 ± 7	41 ± 6	720 ± 74	SP4	3.0	69 ± 6	41 ± 5	873 ± 76	WA	32	45	412
	7.8	38 ± 5	42 ± 5	740 ± 76		6.5	60 ± 4	43 ± 5	717 ± 80	SLP	70	_	734
	10.5	40 ± 8	48 ± 7	817 ± 84		9.5	57 ± 3	43 ± 6	776 ± 82	В	69	102	1014
	14.3	37 ± 7	45 ± 6	755 ± 78		12.5	48 ± 4	44 ± 6	797 ± 83	U	16	39	481
	17.8	33 ± 6	44 ± 6	767 ± 79		15.8	53 ± 4	44 ± 6	807 ± 78				
	20.0	28 ± 6	47 ± 6	783 ± 81		18.5	47 ± 5	43 ± 5	743 ± 91				
	22.8	27 ± 4	48 ± 7	768 ± 79		20.8	48 ± 4	43 ± 6	879 ± 88				
	26.8	33 ± 6	50 ± 7	758 ± 78		23.3	52 ± 6	42 ± 5	856 ± 88				
	29.8	29 ± 6	44 ± 6	708 ± 66		28.3	55 ± 6	43 ± 7	857 ± 83				
	39.3	23 ± 5	48 ± 8	636 ± 51		33.5	56 ± 6	41 ± 6	804 ± 85				
	48.5	26 ± 4	44 ± 6	577 ± 73		44.8	38 ± 4	39 ± 5	828 ± 83				

nearly three weeks before analysis to ensure that secular equilibrium had been achieved. The spectra were taken inside an EG&G Ortec low-background chamber in the range of 100 keV to 1.5 MeV, using a GMX10 gamma EG&G Ortec detector with a standard electronic chain and a 8192 channels multichannel. Energy calibration was performed with ⁶⁰Co, ¹³³Ba, ¹³⁷Cs and ¹⁵²Eu sources. The efficiency calibration was carried out using an admixture of known amounts of naturally occurring ¹⁷⁶Lu (99.9% purity) and ¹³⁸La (99.99% purity) dispersed in a soil substrate (Perillo et al., 1997). The attenuation coefficient of different soils was determined by gamma ray attenuation (Demir et al., 2008; Montes et al., 2009) to ensure that auto-absorption effects were similar for all samples. According to the attenuation coefficient determinations (Montes et al., 2009), we estimate that any remaining water content in the samples could contribute only a variation of $\approx 5\%$ of the attenuation coefficients, which is approximately half the uncertainty of the experimental efficiency curve

The laboratory background was determined and peak corrections were performed. The spectra were recorded during four days and analyzed with a commercial program.

 226 Ra activity of the samples was determined via its daughters 214 Pb and 214 Bi. 232 Th chain activity was determined from the activity of 208 Tl, 212 Bi, 212 Pb and 228 Ac. The 40 K activity was determined using the well-known 1460.75 keV line.

The equilibrium between the 226 Ra and 238 U was evaluated using both, the unresolved 186.21 keV and 185.71 keV peaks from the 226 Ra and 235 U gamma transitions, respectively (Ebaid et al., 2005) and those peaks from 214 Pb and 214 Bi gamma transitions. The 226 Ra activity was calculated assuming that the samples exhibited the 235 U and 238 U natural isotopic abundance, i.e., the 235 U activity ($A_{238}U$) is 0.0462 times the 238 U activity ($A_{238}U$). In addition, the total count rate of the 186 keV peak (C_T) is equal to the sum of the 235 U count rate ($C_{235}U$) and the 226 Ra one ($C_{226}Ra$),

$$C_T = C_{235U} + C_{226Ra} = C_{235U} \left(1 + \frac{C_{226Ra}}{C_{235U}} \right)$$
 (1)

anc

$$C_{235U} = A_{235U} P_{235U}^{\gamma} \varepsilon C_{226Ra} = A_{226Ra} P_{226Ra}^{\gamma} \varepsilon$$
 (2)

being,

$$C_{226Rq} = 0.576C_T \tag{3}$$

where $A_{^{226}Ra}$ is 226 Ra activity, ε the full peak efficiency at 186 keV and $P_{^{235}U}^{\gamma}$ and $P_{^{226}Ra}^{\gamma}$ the gamma ray emission rate for 235 U and 226 Ra transitions, respectively.

Mössbauer spectra were recorded at room temperature (RT) in a 512 channels conventional constant acceleration spectrometer with a 57 CoRh source of approximately 5 mCi nominal activity. Velocity calibration was performed with a 12 μ m thick α -Fe foil at RT. Isomer shifts are referred to this standard. The Mössbauer spectra were numerically analyzed using hyperfine magnetic field and quadrupole splitting distributions (Lagarec and Rancourt, 1998).

RT hysteresis loops where taken using a LakeShore 7404 magnetometer, with fields between 1200 mT and 1200 mT. The saturation magnetization was obtained after subtracting the high-field susceptibility contribution. AC magnetic susceptibility was taken using a LakeShore 7130 susceptometer in the temperature range from 15 to 300 K.

3. Results and discussion

3.1. Radioactivity measurements

The main detected natural activity in all cases originated in 40 K. Table 2 shows that the 232 Th and 226 Ra activities are of the same

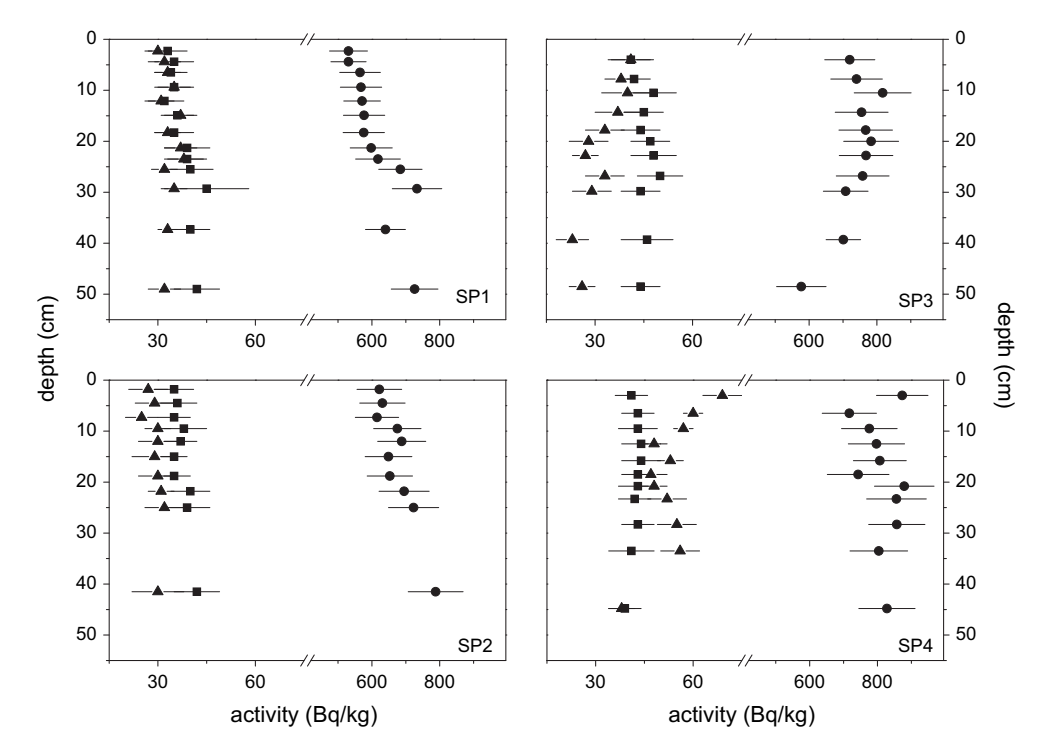


Fig. 2. Activity profiles of ²²⁶Ra, ²³²Th and ⁴⁰K nuclides in SP1, SP2, SP3, and SP4 soils. Circles indicate ⁴⁰K activity while triangles and squares are used to denoted ²²⁶Ra and ²³²Th activity, respectively.

order of magnitude. It is worth mentioning that from the analysis of the spectra and the activity determined data of the different daughters of ²³²Th (²²⁸Ac, ²¹²Pb and ²¹²Bi+²⁰⁸Tl) it is possible to infer that the ²³²Th chain is in equilibrium. In the case of ²²⁶Ra, the activity data obtained from the counts in the 186 keV peak of ²²⁶Ra and ²³⁵U using eq. (3) (Ebaid et al., 2005) and those obtained from the peaks at ²¹⁴Pb and ²¹⁴Bi match well, within the experimental errors (20% and 10%, respectively), suggesting that the equilibrium between ²²⁶Ra and ²³⁸U indeed had been reached. The anthropogenic ¹³⁷Cs was also detected in the soil column; these results are not shown here and will be discussed in a separate article. However, it is worth mentioning that the activity values correspond to those expected from the fallout of the southern hemisphere nuclear weapon tests (UNSCEAR, 2008).

The ⁴⁰K, ²²⁶Ra and ²³²Th activity profiles of SP1, SP2, SP3, and SP4 soils are shown in Fig. 2. In all cases, the determined ²³²Th activities remain constant in depth and space with an average activity concentration equal to 40 ± 4 Bq/kg. 226 Ra activity profiles of SP1and SP2 soils are constant in depth, with mean activities of 34 ± 4 Bq/kg and 29 ± 3 Bq/kg, respectively. On the contrary, the ²²⁶Ra activity for the SP3 and SP4 soil decreases with depth, from 41 ± 3 Bq/kg at the surface to 26 ± 3 Bq/kg at 50 cm of depth for SP3, and from 69 \pm 4 Bq/kg at the surface to 38 \pm 3 Bq/kg at 45 cm of depth for SP4. The ⁴⁰K activity profiles (Fig. 2) are quite different when comparing the four sites. In the SP1 and SP2 profiles, the activity increases with depth for the entire soil column, whereas for SP3 soil the ⁴⁰K activity increases up to 20 cm of depth, and then it decreases. The ⁴⁰K profile observed in the SP4 shows scattered activities. The scattered activities data of ²²⁶Ra and ⁴⁰K of the SP4 profile could be related to the yearly floods of the lowland in this soil (Imbellone et al., 2009).

The surface activity data of ⁴⁰K, ²²⁶Ra and ²³²Th, presented in Table 2, are compared in Fig. 3. Differences are detected, the soils near the coast (SP3, SP4, and SS4) present higher ²²⁶Ra and ⁴⁰K activity concentrations than those soils far from the coast (SP1, SP2, SS1, SS2, SS3, SS5, SS6, SS7 and SS8). Regarding this point, it is widely documented that radionuclides are adsorbed onto clay surfaces or fixed within the lattice structure (Navas et al., 2002). So, the higher activity in the coastal soils may be attributed to a major fixation of the radionuclides because of the major clay fraction (Gimenez et al., 2005; Hurtado et al., 2006a; 2006b).

As observed in Fig. 3 and Table 2, the surface activities determined for the Ezeiza region of the Province of Buenos Aires are similar to those observed in La Plata region. Therefore, the presence of the Atomic Center does not seem to affect the activity concentration of the natural radionuclides studied here.

In Fig. 3, the surface activity data obtained in this work are compared with the average activity values reported for the central region of Argentina (Jury Ayub, 2008), Brazil (Malanca et al., 1996), Uruguay (Odino Moure, 2010) and the worldwide average values (UNSCEAR, 2008), indicated in Table 2. Regarding the ²²⁶Ra activities, the results of SP4 and SS4 soils are close to the average value of Brazil and to those reported for the central region of Argentina, whereas the rest of the soils exhibit activities between those reported for Uruguay and worldwide data. The ²³²Th activities are quite similar to those reported for the central part of Argentina, Uruguay and the worldwide values, while the mean values in Brazil are considerably higher. ⁴⁰K activities have intermediate values between the worldwide and Brazil average

3.2. Activity correlations

A further analysis of the present data and correlation studies between 40 K, 226 Ra and 232 Th was performed by determining the

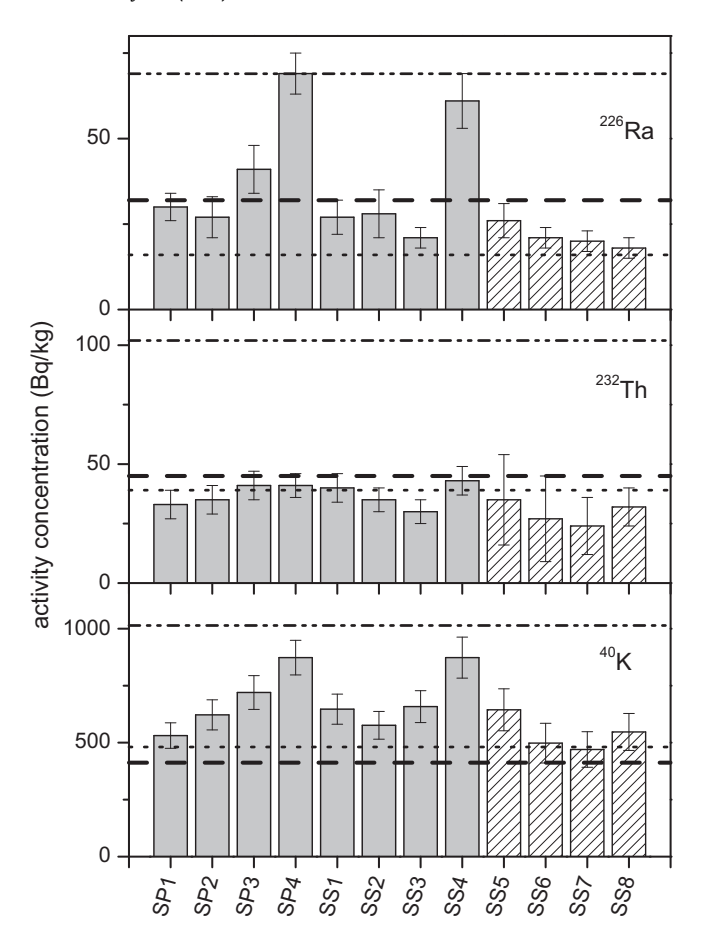


Fig. 3. Comparison of the surface 40 K, 232 Th and 226 Ra activities. Dash line represents the average worldwide activities, dash dot and dot lines represent the average activities in soils of Brazil (Malanca et al., 1996) and Uruguay (Odino Moure, 2010), respectively.

Pearson correlation coefficients (see Table 3). A positive correlation is established among all radionuclides. These values are similar to those determined for Central Spanish Pyrenees soils (Navas et al., 2002) and to those established for anthrosol soils of Belgrade region of Serbia (Vukasinovic et al., 2010). Putting together the present data, the activity soil data reported by UNSCEAR (UNSCEAR, 2000, 2008) and those determined in South American soils (Jury Ayub et al., 2008; Odino Moure, 2010) (see Fig. 4) we calculated once more the Pearson correlation coefficients (global in Table 3). Again, a positive correlation is observed between activities of the radionuclides. Globally, the correlation between ²²⁶Ra and ⁴⁰K decreases approximately 25% with respect to the relation found for Buenos Aires Province, whereas the correlation coefficient value between ⁴⁰K and ²³²Th does not change significantly.

Table 3Pearson correlation matrix of ⁴⁰K, ²³²Th and ²²⁶Ra radionuclide activities. Left: present work. Right: Global data including the present results, UNSCEAR (UNSCEAR, 2008), San Luis province, Argentina (Juri Ayub et al., 2008) and Uruguay (Odino Moure, 2010) data.

Present	work			Global			
	²²⁶ Ra	²³² Th	⁴⁰ K		²²⁶ Ra	²³² Th	⁴⁰ K
²²⁶ Ra	1	0.24	0.59	²²⁶ Ra	1	0.54	0.44
²³² Th	0.24	1	0.65	²³² Th	0.54	1	0.62
⁴⁰ K	0.59	0.65	1	⁴⁰ K	0.44	0.62	1

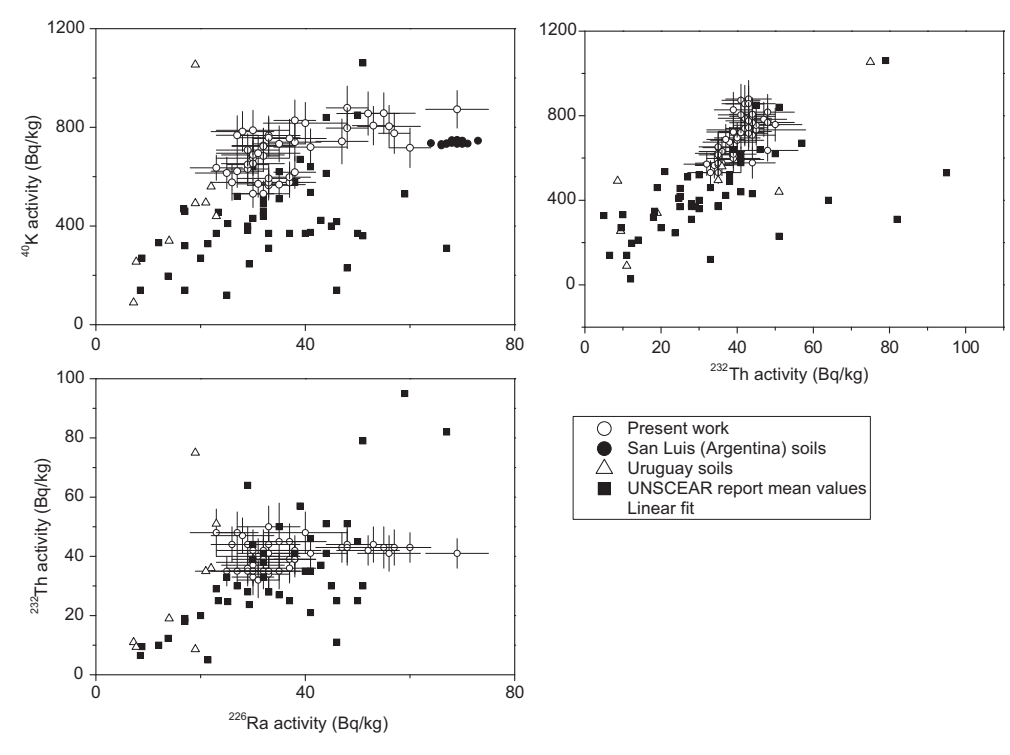


Fig. 4. Correlation between activity concentrations of ²²⁶Ra, ²³²Th and ⁴⁰K, in Bq/kg.

3.3. Magnetic and Mössbauer hyperfine characterization

Fig. 5 shows representative RT Mössbauer spectra recorded for the four soils at different depths. Two main contributions to the spectral area are observed; magnetic sextets and a central set of doublets. To help assign the magnetically split sextets, AC magnetic susceptibility

at different temperatures and RT hysteresis loops were measured for some samples. Samples of inland soils displayed a thermal dependence typical of the mixture of two magnetic phases, whose shape allowed us to assign Verwey and Morin transitions, which are characteristic of magnetite and hematite, respectively. Moreover, the saturation magnetization of the soil samples, with a mean value of

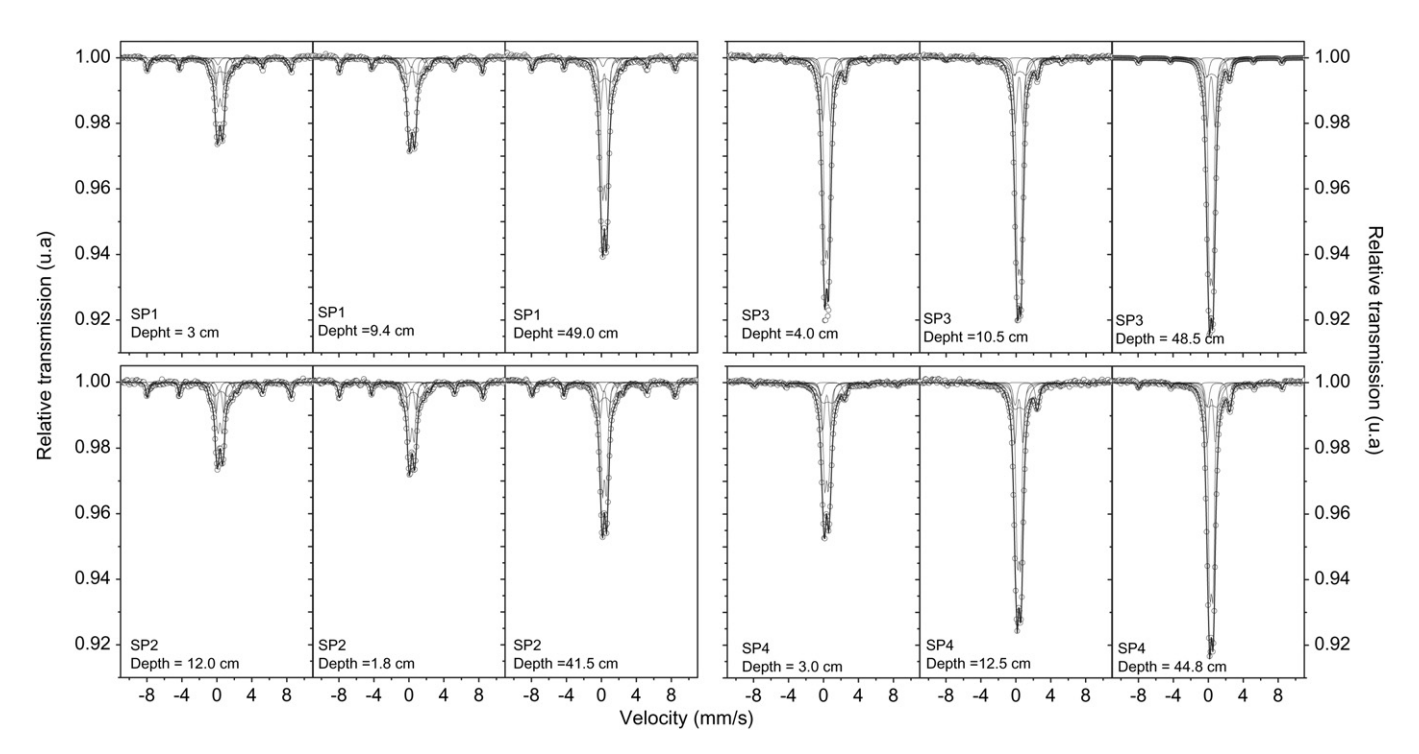


Fig. 5. Selected room temperature Mössbauer spectra labeled with the code sample and depth. The thick solid line is the result of the fitting as describe in the text. Thinner lines correspond to the components shown in Table 4.

Table 4 Hyperfine parameters obtained after fitting the SP1, SP2, SP3 and SP4 Mössbauer spectra using an extended Voigt- based fitting method. Average values of isomer shift 'δ' (mm/s) referred to α-Fe, quadrupole splitting 'Δ' (mm/s), average magnetic field 'B' (T), quadrupole shift ε (mm/s) and relative area rf (%) are listed. PRM: paramagnetic relaxation.

Sample	Depth	Fe ³⁺ (I)			Fe ³⁺ (II)			Fe ²⁺			$\alpha{-}Fe_2O_3$				Fe_3O_4	PMR		
code		δ	Δ	rf	δ	Δ	rf	δ	Δ	rf	δ	ε	Н	rf	rf	ε	Н	rf
SP1	2.3	0.36	0.46	29 ± 2	0.34	0.88	19 ± 3	1.27	2.31	6 ± 1	0.39	-0.11	51.1	15 ± 1	8 ± 3	0.44	6	23 ± 3
	4.4	0.36	0.47	29 ± 7	0.34	0.87	20 ± 6	1.37	2.22	7 ± 2	0.40	-0.12	51.1	14 ± 3	7 ± 4	0.41	6	23 ± 4
	9.4	0.36	0.47	30 ± 2	0.35	0.88	19 ± 3	1.31	2.14	7 ± 1	0.38	-0.12	50.8	14 ± 2	6 ± 4	0.41	6	23 ± 3
	18.3	0.35	0.46	29 ± 2	0.34	0.88	18 ± 3	1.28	2.27	6 ± 1	0.38	-0.12	51.0	14 ± 2	7 ± 3	0.45	6	26 ± 3
	25.5	0.36	0.46	31 ± 2	0.34	0.88	17 ± 3	1.32	2.27	6 ± 1	0.39	-0.12	51.0	14 ± 1	7 ± 3	0.46	6	25 ± 2
	27.5	0.36	0.43	40 ± 3	0.36	0.87	20 ± 3	1.36	2.20	5 ± 1	0.40	-0.12	51.0	9 ± 1	5 ± 2	0.43	6	20 ± 2
	29.3	0.36	0.41	42 ± 3	0.35	0.86	23 ± 2	1.37	2.25	5 ± 1	0.40	-0.12	50.8	8 ± 1	3 ± 2	0.42	6	19 ± 2
	37.3	0.35	0.42	43 ± 3	0.34	0.88	20 ± 2	1.37	2.21	5 ± 1	0.38	-0.10	51.0	9 ± 1	4 ± 2	0.40	6	20 ± 2
	45.6	0.36	0.42	45 ± 2	0.35	0.88	22 ± 2	1.30	2.25	4 ± 1	0.40	-0.12	50.9	8 ± 1	3 ± 3	0.39	6	18 ± 2
	49.0	0.36	0.42	45 ± 2	0.34	0.88	20 ± 2	1.34	2.31	4 ± 1	0.39	-0.11	50.8	9 ± 1	3 ± 2	0.45	6	20 ± 2
SP2	1.8	0.36	0.48	30 ± 2	0.35	0.91	20 ± 2	1.31	2.13	7 ± 1	0.38	-0.11	51.1	16 ± 2	7 ± 4	0.49	6.3	20 ± 2
	7.3	0.36	0.48	29 ± 3	0.35	0.92	19 ± 3	1.31	2.13	7 ± 1	0.40	-0.11	51.1	18 ± 2	9 ± 3	0.47	6.3	19 ± 2
	12.0	0.36	0.49	34 ± 4	0.35	0.92	17 ± 4	1.32	2.13	6 ± 1	0.39	-0.11	51.0	17 ± 2	6 ± 3	0.48	6.3	21 ± 2
	21.8	0.35	0.45	37 ± 4	0.34	0.90	17 ± 3	1.32	2.20	6 ± 1	0.39	-0.10	51.0	15 ± 2	5 ± 3	0.42	6.5	18 ± 2
	29.0	0.36	0.45	46 ± 2	0.34	0.96	14 ± 2	1.36	2.29	5 ± 1	0.38	-0.11	51.0	10 ± 2	6 ± 2	0.42	5.5	20 ± 2
	35.5	0.36	0.45	46 ± 2	0.35	0.96	15 ± 2	1.36	2.29	5 ± 1	0.38	-0.11	50.9	11 ± 1	4 ± 2	0.40	6.0	20 ± 2
	41.5	0.36	0.45	44 ± 1	0.34	0.96	16 ± 1	1.36	2.29	5 ± 1	0.38	-0.11	50.9	11 ± 1	5 ± 2	0.43	6.0	19 ± 1
SP3	4.0	0.36	0.38	54 ± 2	0.36	0.90	21 ± 2	1.16	2.56	8 ± 1	0.40	-0.09	50.6	3 ± 1		0.42	6	14 ± 2
	10.5	0.36	0.36	56 ± 1	0.36	0.90	22 ± 1	1.16	2.58	7 ± 1	0.36	-0.14	50.7	2 ± 1		0.43	6	13 ± 2
	17.8	0.36	0.37	57 ± 1	0.36	0.90	22 ± 1	1.16	2.64	6 ± 1	0.44	-0.09	50.9	2 ± 1		0.45	6	13 ± 1
	22.8	0.35	0.37	58 ± 1	0.36	0.94	20 ± 1	1.15	2.62	7 ± 1	0.36	-0.10	50.8	2 ± 1		0.43	6	13 ± 1
	29.8	0.36	0.37	56 ± 2	0.35	0.92	20 ± 1	1.18	2.55	7 ± 1	0.37	-0.15	51.1	2 ± 1		0.44	6	15 ± 2
	34.3	0.36	0.37	57 ± 2	0.36	0.95	21 ± 1	1.17	2.59	7 ± 1	0.37	-0.13	51.1	2 ± 1		0.42	7	12 ± 2
	39.3	0.36	0.37	56 ± 2	0.36	0.94	21 ± 1	1.18	2.59	7 ± 1	0.37	-0.12	50.9	2 ± 1				
	48.5	0.36	0.37	56 ± 2	0.36	0.93	22 ± 1	1.19	2.56	7 ± 1	0.35	-0.10	50.9	3 ± 1				
SP4	3.0	0.36	0.42	44 ± 2	0.37	0.94	22 ± 2	1.09	2.69	7 ± 1	0.41	-0.10	50.8	4 ± 1		0.50	6	23 ± 3
	6.5	0.36	0.43	44 ± 1	0.38	1.00	22 ± 1	1.11	2.71	8 ± 1	0.38	-0.10	51.0	1 ± 1		0.43	6	25 ± 2
	12.5	0.36	0.39	51 ± 2	0.35	0.93	20 ± 1	1.19	2.55	9 ± 1	0.38	-0.10	50.2	1 ± 1		0.42	6	20 ± 1
	18.5	0.36	0.40	52 ± 1	0.36	0.97	20 ± 1	1.17	2.63	8 ± 1	0.37	-0.10	48.7	1 ± 1		0.39	6	18 ± 1
	23.3	0.36	0.37	55 ± 1	0.34	0.94	20 ± 1	1.21	2.54	7 ± 1	0.37	-0.10	50.7	2 ± 1		0.44	6	16 ± 1
	28.3	0.36	0.38	53 ± 1	0.35	0.91	21 ± 1	1.17	2.59	7 ± 1	0.39	-0.10	51.1	2 ± 1		0.42	6	16 ± 1
	33.5	0.36	0.38	53 ± 1	0.35	0.94	19 ± 1	1.17	2.57	8 ± 1	0.37	-0.11	51.1	2 ± 1		0.41	6	18 ± 1
	40.0	0.36	0.43	53 ± 1	0.37	1.05	18 ± 1	1.14	2.65	9 ± 1	0.38	-0.10	50.4	1 ± 1		0.44	6	19 ± 2
	44.8	0.36	0.38	54 ± 1	0.35	0.93	18 ± 1	1.17	2.57	8 ± 1	0.38	-0.12	50.9	3 ± 1		0.44	6	17 ± 1

58 mAm²/kg and 14 mAm²/kg for inland and costal soils, respectively, reinforces the presence of magnetite in the inland region.

Accordingly, the Mössbauer sextets were fitted assuming three signals; one for hematite, $I_{\alpha-\text{Fe}203}$: B=51.1 T, $\varepsilon=-0.11$ mm/s,

 $\delta=0.39$ mm/s (Vandenberghe, 1991), and two for magnetite, B=49.1 T, $\varepsilon=0.00$ mm/s, $\delta=0.28$ mm/s, B=46.0 T, $\varepsilon=0.00$ mm/s, $\delta=0.66$ mm/s (Murad, 2010). The relative spectral areas varied from sample to sample, and some profiles did not support the

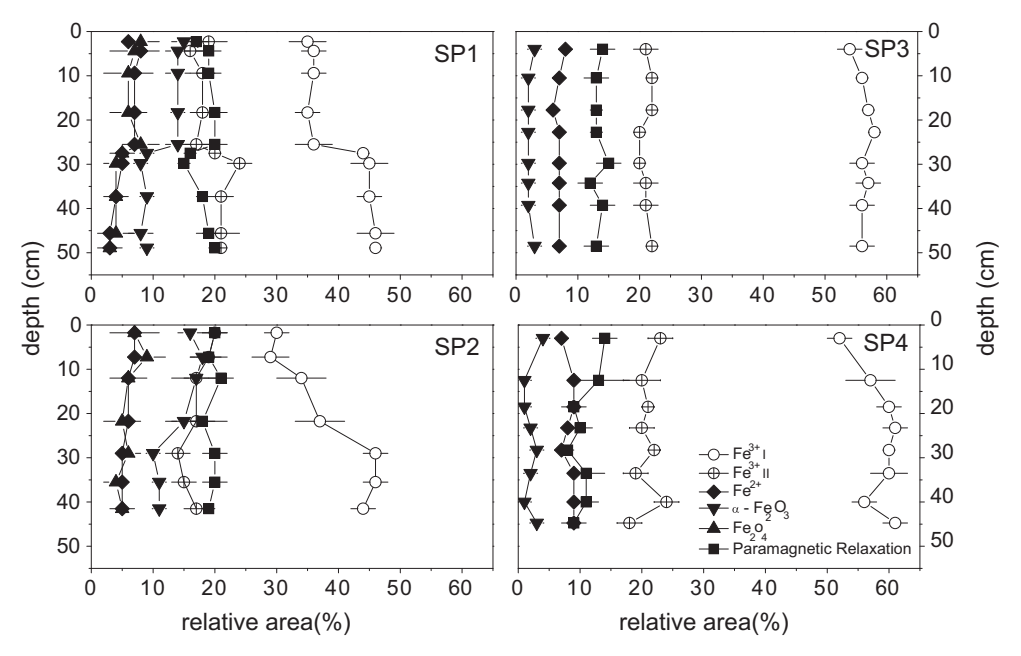


Fig. 6. Evolution of the Mössbauer relative areas of the different Fe surroundings corresponding to the studied profiles.

Table 5 Pearson correlation matrix of 40 K activity and Fe Mössbauer relative areas.

	²²⁶ Ra	²³² Th	⁴⁰ K
α-Fe ₂ O ₃	-0.51	-0.790	-0.633
Fe ₃ O ₄	-0.51	-0.800	-0.682
Fe ³⁺ (I)	0.27	0.842	0.640
Fe ³⁺ (II)	0.18	0.495	0.102
Fe ³⁺ tot	0.723	0.891	0.562
Fe ²⁺	0.08	0.094	0.233

existence of magnetite. Although Mössbauer spectra taken at room temperature do not allow determining accurately the magnetic species contributing to the spectral area, they are able to sense the existence of one or two magnetic phases. Because of the presence of fine particles in the soil samples, the broad lines of the spectra produced by the fine particles of the soil samples made it reasonable to perform the fittings assuming hyperfine field distributions. To account for the total spectrum, superimposed to the above mentioned sextets, it was necessary to include two quadrupole split doublets associated to paramagnetic Fe³⁺ species $\Delta = 0.46$ mm/s, $\delta = 0.36$ mm/s, $\Delta = 0.88$ mm/s, $\delta = 0.34$ mm/s), a Fe²⁺ species ($\Delta = 2.31 \text{ mm/s}, \delta = 1.27 \text{ mm/s}$) and a paramagnetic relaxation $(B = 6.0 \text{ T}, \varepsilon = 0.00 \text{ mm/s}, \delta = 0.44 \text{ mm/s})$ (Murad, 2010; Paduani, et al., 2009). The fitted parameters are quoted in Table 4 together with the corresponding relative areas. Because of the overlapping of different Fe species with similar parameters (Paduani, et al., 2009; MacCammon, 1995), the assignment of the Mössbauer parameters of the doublets to iron compounds is uncertain. Based on low-temperature previous results (Montes et al., 2010), the determined quadrupole interactions could be related to the Fe³⁺ and the Fe²⁺ ions existing at the octahedral and tetrahedral sites in paramagnetic phases (MacCammon, 1995; Murad, 1998; Paduani, et al., 2009).

The evolution of the relative areas of the different Fe surroundings with depth is shown in Fig. 6. It is observed that for all

samples, independently of depth, the main component corresponds to the $\text{Fe}^{3+}(I)$ doublet. However, the relative fractions of the Fe phases differ for soil samples of different locations. In the coastal area soils (SP3 and SP4), the relative areas are nearly constant in depth, Fe_3O_4 was not detected and the $\alpha\text{-Fe}_2\text{O}_3$ contribution is lower than the corresponding to the SP1 and SP2 soils. The Fe^3+ fractions of inland soils (SP1 and SP2) increase up to 82%, mainly at the expense of the $\alpha\text{-Fe}_2\text{O}_3$ spectral area. The paramagnetic relative area for coastal soils is higher than those for inland soils. This fact is also reflected in the high-field magnetization determined by the hysteresis loops, with a mean value of 12 \times 10 $^{-8}$ m³/kg and 4×10^{-8} m³/kg for coastal and inland soils, respectively. For all soils, the Fe²+ fraction profile is constant in depth.

3.4. Correlation between activity radionuclides and iron species

As it is well-known, the distribution of radionuclides in the geosphere depends on the distribution of the geological media from which they are derived and the processes which concentrate them at a specific region. The key to understanding these distributions, therefore, is to know the distribution of the source materials and the physical and geochemical processes that lead to elevated concentrations of radionuclides under specific conditions. In the process of mineral formation, the radionuclides are incorporated as trace elements in the crystal lattice. The concentration of these elements depends on the type of mineral and abundance in the parent magma. In both cases, the minerals and the radionuclides can be assumed to be dispersedly present and if they are similarly affected by the erosive processes, correlation between the mayor minerals and the radionuclides may be expected (Suresh et al., 2011).

Putting together the natural radiological and hyperfine characterization of Fe species content of soils, it was observed that the coastal soils without magnetite and lower hematite relative area presented a higher ²²⁶Ra and ⁴⁰K activities. Indeed, the obtained Pearson correlation coefficients, quoted in Table 5, indicate

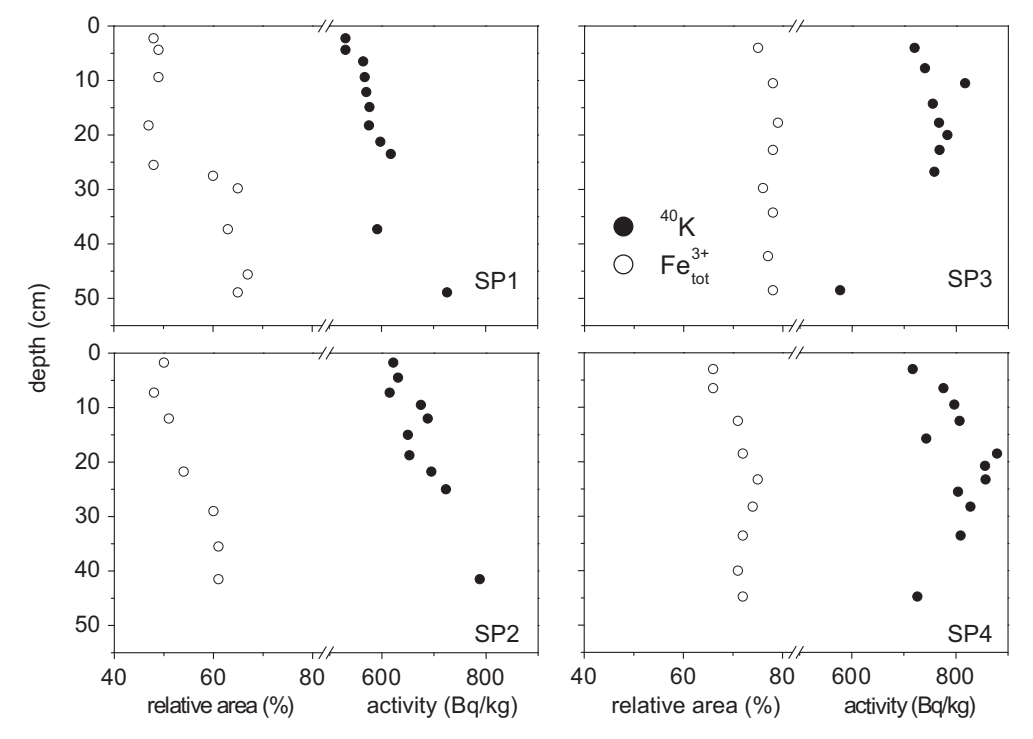


Fig. 7. 40 K activity vs. Fe^{3+} total relative area ($Fe^{3+}(I) + Fe^{3+}(II)$) labeled with the sample code.

Table 6Calculated annual committed effective dose (ACED) for infants, children and adults.

Sample code	Calculated ACED (mSv)							
	Infants	Children	Adults					
SP1	0.085 ± 0.009	0.078 ± 0.007	0.068 ± 0.007					
SP2	0.095 ± 0.009	0.083 ± 0.008	0.073 ± 0.007					
SP3	0.120 ± 0.010	0.102 ± 0.009	0.090 ± 0.008					
SP4	0.140 ± 0.010	0.120 ± 0.009	0.106 ± 0.008					
SS1	0.102 ± 0.009	0.088 ± 0.008	0.078 ± 0.007					
SS2	0.093 ± 0.009	0.081 ± 0.008	0.071 ± 0.007					
SS3	0.089 ± 0.009	0.077 ± 0.008	0.068 ± 0.007					
SS4	$\textbf{0.140} \pm \textbf{0.010}$	0.130 ± 0.010	0.110 ± 0.009					
Average	0.11 ± 0.01	0.94 ± 0.01	0.083 ± 0.007					
SS5	0.10 ± 0.02	0.08 ± 0.02	0.07 ± 0.02					
SS6	0.07 ± 0.02	0.07 ± 0.02	0.06 ± 0.01					
SS7	0.07 ± 0.02	0.06 ± 0.01	0.05 ± 0.01					
SS8	$\textbf{0.08} \pm \textbf{0.01}$	0.07 ± 0.01	0.06 ± 0.01					
Average	0.08 ± 0.02	0.07 ± 0.02	0.06 ± 0.02					

a negative correlation between the radionuclide activities and the Mössbauer relative areas. Moreover, as observed in Fig. 7, the Fe^{3+} total relative fraction ($Fe^{3+}(I) + Fe^{3+}(II)$) and the 40 K activity profile in SP1 and SP2 soils have quite similar behavior. Regarding the above mentioned soil texture (Gimenez et al., 2005; Hurtado et al., 2006a; 2006b) and considering the paramagnetic signals used for

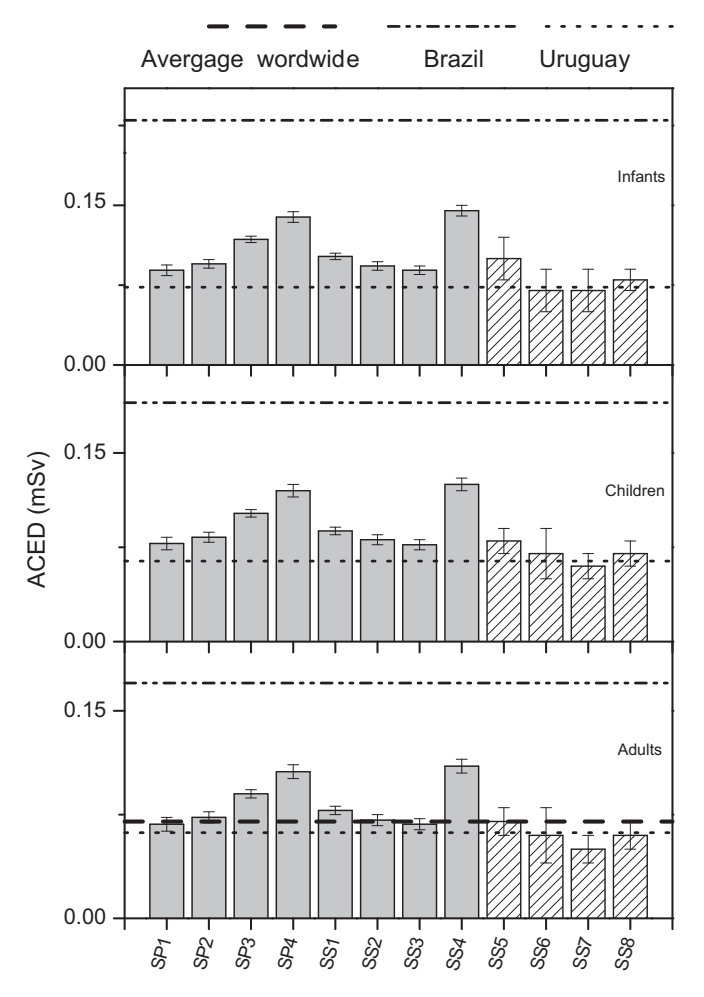


Fig. 8. Calculated annual committed effective dose for infants, children and adults. The vertical bars correspond to the experimental errors. The dash line represent the average worldwide value (UNSCEAR, 2008), the dot line is Uruguay dose calculated from Odino Moure (2010) activity data and dash dot line is calculated dose from Brazil soils activity reported by Malanca et al. (1996).

the Mössbauer spectra fitting procedure, it is tempting to assign the origin of these interactions to illite phase, while minor contributions to the spectra of other phases cannot be completely discarded. With this picture in mind, the correlation found between the ⁴⁰K activity and the Fe³⁺ relative fractions could be interpreted as the trapping of these ions by illite. Moreover, it has been previously suggested that the K content in soils can be considered as an indicator of the content of micaceous clay (Laubenstein and Magaldi, 2008; Barré et al., 2008; Hinsinger, 2002), reinforcing this hypothesis.

3.5. Dose calculations

There is a direct relationship between terrestrial gamma radiation and radionuclide concentrations in soils (UNSCEAR, 2000, 2008). The exposure dose rate at 1 m above the ground can be evaluated taking into account the activity values of the radionuclides and the conversion factors of ²³⁸U, ²³²Th and ⁴⁰K (UNSCEAR, 2000; UNSCEAR, 2008). The coefficient to convert the absorbed dose in air to annual committed effective dose (ACED) values were taken from reference (UNSCEAR, 2000). To calculate the annual effective doses it has also been considered that the ²³⁸U. ²²⁶Ra and its daughter are in secular equilibrium and that the spent time outdoors is 20% of the total time (UNSCEAR, 2008). In Table 6 the calculated doses for infants, children and adults are reported. As it can be seen from Fig. 8, the reported doses are quite similar for the studied region. On the other hand, the average calculated doses for Brazil are higher than those for La Plata city and Ezeiza regions. However, comparing with the average doses of Uruguay, the values for Argentina are higher. It is worth mentioning that in the case of adults, the calculated annual committed effective doses due to terrestrial external exposure were similar to the UNSCEAR reported values (UNSCEAR, 2000).

4. Conclusions

In the frame of an ambitious project focused on the study of the soils of the Province of Buenos Aires, Argentina, the natural activity concentration profiles of ⁴⁰K, ²²⁶Ra and ²³²Th chain were assessed for soils from La Plata and Ezeiza regions. This work is the first study carried out in the Province of Buenos Aires, where a nuclear power plant is in operation, a second one will be active soon, and there is a nuclear center with research and radionuclide production reactor, a plant for nuclear fuel production and facilities for nuclear waste management.

The activities of 226 Ra and 40 K determined in the coastal area were higher than the activities found for the inland soils. Taking into account all the reported 40 K and 226 Ra worldwide soil activity data, we conclude that there is a positive correlation between these radionuclides.

The simultaneous analysis of the activity and the Mössbauer data has enabled us to find a negative correlation between the activity concentration of all determined natural radionuclides and the magnetite and hematite relative fractions, with Pearson correlation coefficient ranging from -0.5 to -0.80. Moreover, a positive correlation (0.56) was observed between the paramagnetic Fe³⁺ relative areas and ⁴⁰K, reinforcing the hypothesis that K is highly related to the existence of micaceous minerals. To our knowledge, this is the first investigation that has taken into account the correlation between the Mössbauer hyperfine parameters and the radioactivity of natural radionuclides found in soils.

The annual committed effective dose determined for La Plata and Ezeiza regions are similar, and analogous to the UNSCEAR reported values.

Acknowledgements

Research grants PIP 0230 from Consejo Nacional de Investigaciones Científicas y Técnicas (CONICET, Argentina) and PICT 38047-Préstamo BID from Agencia de Promoción Científica (ANCYT, Argentina) are gratefully recognized.

References

- Juri Ayub, J., Velasco, R.H., Rizzotto, M., Quintana, E., Aguiar, J., 2008. In: Paschoa, A.S. (Ed.), ⁴⁰K, ¹³⁷Cs and ²²⁶Ra Soil and Plant Content in Semi-natural Grasslands of Central Argentina. The Natural Radiation Environment—8th International Symposium. American Institute of Physics.
- Barré, P., Velde, B., Fontaine, C., Catel, N., Abbadie, L., 2008. Which 2:1 clay minerals are involved in the soil potassium reservoir? Insights from potassium addition or removal experiments on three temperate grassland soil clay assemblages. Geoderma 146, 216—223.
- CNEA, 2011. http://www.cnea.gov.ar/xxi/cnea_info/cae.asp.
- Demir, D., Un, A., Ozgul, M., Sahin, Y., 2008. Determination of photon attenuation coefficient, porosity and field capacity of soil by gamma ray transmition for 60 KeV, 356 KeV and 662 KeV gamma rays. Applied Radiation and Isotopes 12 1984–1837.
- Ebaid, Y.Y., El-Mongy, S.A., Allam, K.A., 2005. ²³⁵U-γ emission contribution to the 186 keV energy transition of ²²⁶Ra in environmental samples activity calculations. International Congress Series 1276, 409–411.
- Gimenez, J.E., Cabral, M.G., Hurtado, M.A., 2005. Elaboración y Transferencia de cartografía Temática e Implementación de un Sistema de Información Geográfica para el Planeamiento (Partido de Berisso). Comisión de Investigaciones Científicas de la Provincia de Buenos Aires. Universidad Nacional de La Plata.
- Hinsinger, P., 2002. Potassium. In: Lal, R. (Ed.), Encyclopedia of Soil Science. Marcel Dekker, Inc., New-York, USA.
- Hurtado, M.A., Gimenéz, J.E., Cabral, M.G., 2006a. Análisis ambiental del partido de La Plata. Aportes al ordenamiento territorial. Consejo Federal de Inversiones. Universidad Nacional de La Plata.
- Hurtado, M.A., Gimenéz, J.E., Cabral, M.G., 2006b. Suelos del partido de Berazategui como base para el planeamiento ambiental y ordenamiento territorial. Contrato de Obra entre Consejo Federal de Inversiones y Facultad de Ciencias Naturales y Museo. Universidad Nacional de La Plata.
- IAEA, 2003. Applicability of Monitored Natural Attenuation at Radioactively Contaminated Sites. Technical Reports Series No. 445, Vienna.
- Imbellone, P.A., Guichon, B.A., Giménez, J.E., 2009. Hydromorphic soils of the Rio de la Plata coastal plain, Argentina. Latin Amercan Journal of Sedimentology and Basin Analysis 16, 3—18.
- Perillo Isaac, M.C., Hurley, D., McDonald, R.J., Norman, E.B., Smith, A.R., 1997. A natural calibration source for determining germanium detector efficiencies. Nuclear Instruments and Methods in Physics Research A397, 310–316.

- Lagarec, K., Rancourt, D.G., 1998. Mössbauer Spectral Analysis Software, Version 1.05. Department of Physics, University of Ottawa.
- Laubenstein, M., Magaldi, D., 2008. Natural radioactivity of some red Mediterranean soils. Catena 76, 22–26.
- MacCammon, C.A., 1995. Mössbauer Spectroscopy of Minerals in Mineral Physics & Crystallography: Hanndbook of Physical Constants. American Geophysical Union, Washington DC. 332–347.
- Malanca, A., Gaidolfi, L., Pessina, V., Dallara, G., 1996. Distribution of ²²⁶Ra, ²³²Th, and ⁴⁰K in soils of Rio Grande do Norte (Brazil). Journal of Environmental Radioactivity 30, 55–67.
- Megumi, K., Oka, T., Doi, M., Kimura, S., Tsujimoto, T., Ishiyama, T., Katsurayama, K., 1988. Relationships between the concentrations of natural radionuclides and the mineral composition of the surface soil. Radiation Protection Dosimetry 24, 69–72.
- Montes, M.L., Taylor, M.A., Runco, J., Errico, L., Martines, J., y Desimoni, J., 2009. Implementación de la técnica de espectroscopía gamma para la determinación de humedad en suelos. ANALES AFA 20, 205–207.
- Montes, M.L., Taylor, M.A., Mercader, R.C., Sives, F.R., Desimoni, J., 2010. Hyperfine and Radiological Characterization of Soils of the Province of Buenos Aires. Journal of Physics, Argentina. Conference Series. 217.
- Murad, E., 1998. Clays and clay minerals: what can Mössbauer spectroscopy do to help understand them? Hyperfine Interactions 117, 39–70.
- Murad, E., 2010. Mössbauer spectroscopy of clays, soils and their mineral constituents. Clay Minerals 45, 413–430.
- NASA. 2011. www.na-sa.com.ar.
- Navas, A., Soto, J., Machín, J., 2002. ²³⁸U, ²²⁶Ra, ²¹⁰Pb, ²³²Th and ⁴⁰K activities in soil profiles of the Flysch sector (Central Spanish Pyrenees). Applied Radiation and Isotopes 57, 579–589.
- Odino Moure, M.R., 2010. Environmental Radioactivity Monitoring Plan in Uruguay.

 Technical Meeting on In-situ Methods for Characterization of Contaminated Sites. Austria, Vienna. http://www-pub.iaea.org/mtcd/meetings/Announcements.asp?ConflD=38924.
- Paduani, C., Samudio Pérez, C.A., Gobbi, D., Ardisson, J.D., 2009. Mineralogical Characterization of iron-rich clayey soils from the middle plateau in the southern of Brazil. Applied Clay Science 42, 559–562.
- Suresh, G., Ramasamy, V., Meenakshisundaram, V., Venkatachalapathy, R., Ponnusamy, V., 2011. A relationship between the natural radioactivity and mineralogical composition of the Ponnaiyar river sediments, India. Journal of Environmental Radioactivity 102, 370–377.
- UNSCEAR, 2000. In: Sources and Effects of Ionizing Radiation, Report of the General Assembly with Scientific Annexes, vol. 1 (New York).
- UNSCEAR, 2008. In: Sources and Effects of Ionizing Radiation, Report of the General Assembly with Scientific Annexes, vol. 1 (New York).
- Vandenberghe, R.E., 1991. Mössbauer Spectroscopy and Applications in Geology, International Training Centre for Post-graduate Soil Scientists. Geological Institute, Faculteit der Wetenschappen, Faculty of Science, Belgium.
- Vukasinovic, I., Dordevic, A., Rajkovic, M.B., Todorovic, D., Pavlovic, V., 2010. Distribution of natural radionuclides in anthrosol-type soil. Turkish Journal of Agriculture and Forestry 34, 539–546.